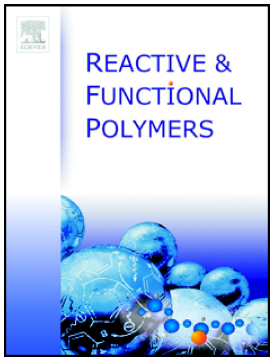

Synthesis and properties of photocross-linkable carbazole dimers

G. Simkus, A. Tomkeviciene, D. Volyniuk, S.V. Kostjuk, J.V. Grazulevicius

PII: S1381-5148(16)30230-9
DOI: doi: 10.1016/j.reactfunctpolym.2016.12.004
Reference: REACT 3778

To appear in: *Reactive and Functional Polymers*

Received date: 16 June 2016
Revised date: 9 November 2016
Accepted date: 2 December 2016

Please cite this article as: G. Simkus, A. Tomkeviciene, D. Volyniuk, S.V. Kostjuk, J.V. Grazulevicius , Synthesis and properties of photocross-linkable carbazole dimers. The address for the corresponding author was captured as affiliation for all authors. Please check if appropriate. React(2016), doi: 10.1016/j.reactfunctpolym.2016.12.004

LISYNTHESIS AND PROPERTIES OF PHOTOCROSS-LINKABLE CARBAZOLE DIMERS

G. Simkus[a], A. Tomkeviciene[a], D. Volyniuk[a], S.V. Kostjuk[b], J.V. Grazulevicius[a]*

[a]*Department of Polymer Chemistry and Technology, Kaunas University of Technology, Radvilenu rd. 19, LT-50254, Kaunas, Lithuania*

[b]*Reaseach Institute for Physical Chemical Problems of the Belarusian State University, Leningradskaya st. 14 220030, Minsk, Belarus*

* Corresponding author. Tel.: +370 37 300193; fax: +370 37 300152. E-mail address: juozas.grazulevicius@ktu.lt (J.V. Grazulevicius).

Abstract

New carbazole-based monomers with two reactive functional groups such as epoxypropyl, oxetanyl and vinyloxethyl were synthesized and their cationic photopolymerization was performed. The monomer containing epoxypropyl groups exhibited the highest conversion in photopolymerization (78 %). The monomers and polymers exhibited ability of glass formation with the glass transition temperatures up to 98 ^{o}C for low-molecular-weight compounds and those observed for polymers ranging from 89 to 150 ^{o}C. The synthesized derivatives absorb electromagnetic irradiation in the range of 200 – 390 nm with the band gaps of 3.14 – 3.16 eV. The compounds exhibit blue photoluminescence with the intensity maxima at 400 nm. The compounds were found to have high triplet energies of ca. 2.78 eV. The electron photoemission spectra of the layers of the synthesized compounds revealed ionization potentials of 5.20 – 5.37 eV. The time-of-flight hole drift mobilities of the layers of the compounds exceed 10^{-5} cm^2/V×s at high electric fields.

Keywords: Carbazole; Glass-forming; Cross-linking, Thermal stability; Charge mobility.

1. Introduction

The current level of development of organic light emitting diodes (OLEDs) enables their effective application in the low-cost flat panel display technology and lighting [1]. Most of OLEDs are the multilayer systems, which are composed of hole-transport, emitting, and electron-transport layers and often some additional layers sandwiched between two electrodes [2,3]. Two methods are popular in their fabrication. The most commonly used one is vacuum deposition. High quality multilayer devices are fabricated by this method, but it is suitable only for low-molar-mass compounds, characterized by high thermal stability. In addition, vacuum deposition also requires high instrumental expenses and time to

prepare solid films which leads to relatively high costs [4]. An alternative method to fabricate multilayer systems is spin-coating. It requires less investments and enables to coat larger areas. However, most of organic semiconductors are soluble in the same organic solvents. Therefore during preparation of multilayer systems it is important to ensure insolubility of a bottom layer onto which a top layer has to be cast. The approach that is used to solve this problem is to render the material insoluble after spin-coating. In order to get insoluble layer soluble functionalized precursor polymers, crosslinkable side-chain polymers or monomers are used [5]. The crosslinking process for obtaining insoluble polymer layers can be carried out using thermal [6,7], photochemical [8-10], or chemical treatment [11,12].

It is well know that carbazole-based darivatives are characterized by high triplet energies, E_T (up to 3.05 eV), excellent hole-transporting properties, wide bang gap and thermal stability which are the main requirements for host materials used in blue phosphorescent OLEDs [13,14]. In this work we report on the synthesis and properties of several photocross-linkable carbazole based monomers and demonstrate their photocross-linking.

2. Experimental

2.1. Instrumentation

^{1}H and ^{13}C NMR spectra were recorded using Bruker Avance III [400 MHz (^{1}H), 100 MHz (^{13}C)] spectrometer at room temperature. All the data are given as chemical shifts in δ (ppm). $(CH_3)_4Si$ (TMS, 0 ppm) was used as an internal standard. The courses of the reactions were monitored by thin layer chromatography (TLC) using Silicagel 60 F254 plates and developed with I_2 or UV radiation. Silica gel (grade 60, 63–200 mesh, 60 Å, Fluka) was used for column chromatography. Melting points (m.p.) of the compounds were determined using Electrothermal Mel-Temp melting point apparatus. Mass (MS) spectra were recorded on a Waters (ACQUITY UPLC®). Elemental analysis was performed with an Exeter Analytical CE-400 Elemental. Differential scanning calorimetry (DSC) measurements were carried out using a DSC Q2000 thermal analyzer at a heating rate of 10 ^oC/min under nitrogen flow. Thermogravimetric analysis (TGA) was performed on a TGA Q50 apparatus.

Absorption spectra of the dilute tetrahydrofuran (THF) solutions were recorded on Perkin Elmer Lambda 35 spectrometer. Room temperature photoluminescence (PL) spectra of the synthesized compounds were taken by Perkin Elmer LS 55 spectrometer. For these measurements, the dilute solutions of the investigated compounds were prepared by dissolving them in a spectral grade THF at 10^{-4} M concentration. The phosphorescence spectra of dilute solution in THF (10^{-4} M) were recorded at 77 K by Edinburgh Instruments FLS980.

The kinetics of the photopolymerization were monitored by real-time FT-IR spectroscopy using Bruker Vertex 70 spectrometer. The samples were exposed by UV radiation with the wavelength range of 250–450 nm using UV/Visible spot curing system OmniCure S2000 (Lumen Dynamics Group Inc). The intensity of the UV radiation was 9.3 $W \cdot cm^{-2}$ (high pressure 200 W mercury vapor short arc).

The cyclic voltammetry (CV) measurements were carried out by a three-electrode assembly cell from Bio-Logic SAS and a micro-AUTOLAB Type III potentiostat-galvanostat. The working electrode was a glassy carbon of 0.12 cm^2 surface. The reference electrode and the counter electrode were Ag/Ag^+ 0.01 M and Pt wire respectively. The solutions with the concentration of 10^{-3} M of the compounds in argon-purged dichloromethane with tetrabulthylammonium perchlorate (TBAP; 0.1M) as electrolyte were used for the CV measurements. The CV curves were drawn versus Fc/Fc^+ as internal reference where the potential of the redox system $E^{Fc}_{1/2}$=0.210 V/Ag:Ag^+.

The ionization potentials ($I_{p(EP)}$) of the solid samples of the synthesized compounds were measured by the electron photoemission spectrometry in air as reported earlier [15]. The measurement error is evaluated as 0.03 eV. The samples for the measurements were prepared by dissolving compounds in THF and by casting on ITO coated glass plates. The experimental setup consisted of deep UV deuterium light source ASBN-D130-CM, CM110 1/8m monochromator, and electrometer 6517B Keithley.

The charge carrier mobility (μ) measurements were carried by the time of flight method (TOF) [16]. The sandwich-like cells (ITO/compound/Al) were fabricated for the measurements. First, the layers of the compounds were prepared by drop casting their solutions in THF onto cleaned ITO coated glass substrate. Finally, Al electrode (80 nm) was evaporated at 15 Å/s. The thickness of thin layers was measured using the method of carrier extraction by linearly increasing voltage (CELIV) (ε~3) [17]. The charge carriers were generated at the layer surface by illumination with pulses of Nd:YAG laser(EKSPLA NL300, a wavelength of 355 nm, pulse duration 3-6 ns). The transit time was determined from the kink point in the transient photocurrent curves. The transit time t_t with the applied bias (V) indicates the passage of holes through the entire thickness of the cell (d) and enables determination of the hole mobility as $\mu=d^2/U \times t_t$. The experimental setup consisted of a Keithley 6517B electrometer, and a Tektronix TDS 3052C oscilloscope.

2.2 Materials

3-Iodo-9*H*-carbazole (**1**) [18], 3,6-dibromo-9*H*-carbazole (**3**) [19] and 3,6-dimethoxy-9*H*-carbazole (**4**) [20] were synthesized according to procedures described in literature. 3-Iodo-9-isopentyl-9*H*-carbazole (**2**) was prepared by alkylation of 3-iodocarbazole in the presence of phase transfer catalyst [21].

3-(3,6-Dimethoxycarbazol-9-yl)-9-isopentylcarbazole (**5**)

A mixture of 3-iodo-9-isopentyl-9*H*-carbazole (3.84 g, 10 mmol), 3,6-dimethoxy-9*H*-carbazole (2 g, 8.8 mmol), 18-crown-6 (0.44 mmol, 0,12 g), potassium carbonate (9.73 g, 71 mmol), and copper powder (2.24 g, 35 mmol) in o-dichlorbenzene (30 ml) was refluxed under argon at 180 ^{o}C. After 4 h the reaction was stopped, copper powder and inorganic salts were removed by filtration. The solvent was distilled under reduced pressure and the crude product was purified by column chromatography on silica gel using hexane/dichloromethane (3/1) as an eluent. The target compound was obtained as brownish powder (fw=462g/mol) in 72 % yield (3.52 g). ^{1}H NMR (400 MHz, $CDCl_3$), δ (ppm): 8.20 (s, 1H, Ar), 8.05 (d, *J* = 7.8 Hz, 1H, Ar), 7.60 (d, *J* = 2.4 Hz, 2H, Ar), 7.56 – 7.54 (m, 2H, Ar), 7.50 (dd, *J* = 7.0, 1.2 Hz, 1H, Ar), 7.45 (d, *J* = 8.2 Hz, 1H, Ar), 7.29 (d, *J* = 8.9 Hz, 2H, Ar), 7.27 – 7.21 (m, 1H, Ar), 7.04 (dd, *J* = 8.9, 2.5 Hz, 2H, Ar), 4.38 (t, *J* = 7.1 Hz, 2H, NCH_2), 3.96 (s, 6H, OCH_3), 1.86 – 1.69 (m, 3H, CH_2, CH), 1.07 (d, *J* = 6.3 Hz, 6H, CH_3). ^{13}C NMR (100 MHz, $CDCl_3$), δ (ppm): 153.8, 140.9, 139.2, 137.5, 130.6, 129.3, 127.8, 126.3, 125.1, 123.7, 123.2, 122.5, 120.7, 119.3, 119.2, 115.2, 110.8, 109.5, 108.9, 102.9, 56.2 (2C, OCH_3), 41.6 (NCH_2), 37.6 (CH), 26.2 (CH_2), 22.7 (2C, CH_3). MS ($APCl^+$, 20 V), *m/z* (%) = 463 ($[M + H]^+$, 100). Elemental analysis. Calcd for $C_{31}H_{30}N_2O_2$ (%): C 80.49, H 6.54, N 6.06, O 6.92; found (%): C 80.54, H 6.56, N 6.09.

*3-(3,6-Dihydroxycarbazol-9-yl)-9-isopentylcarbazole (**6**)*

Compound **5** (1 g, 2.2 mmol) was dissolved in dry dichloromethane (DCM, 15 ml) at room temperature and cooled to -80 ^{o}C. Boron tribromide (1 M in DCM, 11.2 ml, 11.2 mmol) was added slowly. After the addition, the homogeneous mixture was stirred at -80 ^{o}C for 30 min and then it was allowed to warm slowly to room temperature overnight. The reaction mixture was poured into water (200 ml), stirred for 30 min, and extracted with DCM. The combined organic phase was dried over Na_2SO_4, filtered, and concentrated. The crude product was purified by column chromatography on silica gel using hexane/acetone (4/1) as an eluent. The target compound was obtained as white crystals (fw=434 g/mol, m.p.: 131 – 132 ^{o}C) in 85 % yield (0.80 g). ^{1}H NMR (400 MHz, DMSO-d_6), δ (ppm): 9.06 (s, 2H, OH), 8.34 (s, 1H, Ar), 8.23 (d, *J* = 6.8 Hz, 1H, Ar), 7.79 (d, *J* = 8.6 Hz, 1H, Ar), 7.63 (d, *J* = 8.0 Hz, 1H, Ar), 7.56 (dd, *J* = 8.6, 2.1 Hz, 1H, Ar), 7.51 (t, *J* = 7.1 Hz, 1H, Ar), 7.44 (d, *J* = 2.4 Hz, 2H, Ar), 7.21 (t, *J* = 7.7 Hz, 1H, Ar), 7.14 (d, *J* = 8.8 Hz, 2H, Ar), 6.89 (dd, *J* = 8.7, 2.4 Hz, 2H, Ar), 4.47 (t, *J* = 7.1 Hz, 2H, NCH_2), 1.77 – 1.65 (m, 3H, CH_2, CH), 1.01 (d, *J* = 6.1 Hz, 6H, CH_3). ^{13}C NMR (100 MHz, DMSO) δ (ppm): 151.3, 140.9, 138.9, 136.4, 129.5, 126.8, 125.1, 123.5, 123.4, 122.3, 121.5, 119.4, 119.3, 115.7, 110.7, 110.5, 109.8, 105.5, 41.4 (NCH_2), 37.7 (CH), 26.0 (CH_2), 23.0 (2C, CH_3). MS ($APCl^+$, 20 V), *m/z* (%) = 435 ($[M + H]^+$, 100). Elemental analysis. Calcd for $C_{29}H_{26}N_2O_2$ (%): C 80.16, H 6.03, N 6.45, O 7.36; found (%): C 80.22, H 6.08, N 6.48.

*3-(3,6-Di((2,3-epoxypropyl)oxy)carbazol-9-yl)-9-isopentylcarbazole (**7a**)*

Compound **6** (0.5 g, 11.5 mmol), 3-chloro-1,2-epoxypropane (8.5 g, 92 mmol) and benzyltrimethylammonium chloride (BTMA, 0.1 g, 0.58 mmol) were placed in a 250 ml round-bottomed flask. The mixture was heated at reflux for one hour. The excess of 3-chloro-1,2-epoxypropane was removed at reduced pressure, and the resin obtained was dissolved in DCM, washed several times with water and dried over magnesium sulfate. The solvent was evaporated and the residue was purified by column chromatography on silica gel using hexane/ethyl acetate (4/1) as an eluent. The target compound was obtained as yellowish powder (fw=546 g/mol) in 74 % yield (0.47 g). ^{1}H NMR (400 MHz, $CDCl_3$), δ (ppm): 8.19 (s, 1H, Ar), 8.06 (d, J = 7.7 Hz, 1H, Ar), 7.61 (d, J = 2.5 Hz, 2H, Ar), 7.57 – 7.42 (m, 4H, Ar), 7.33 – 7.21 (m, 3H, Ar), 7.07 (dd, J = 8.9, 2.5 Hz, 2H, Ar), 4.40 (t, J = 7.5 Hz, 2H, NCH_2), 4.36 (dd, one of CH_2O protons in oxirane ring ($H_{A'}$), $J_{A'M'}$ = 3.2, $J_{A'X'}$ = 11.0 Hz, 2H), 4.11 (dd, one of another CH_2O protons in oxirane ring ($H_{M'}$), $J_{M'A}$=5.6, $J_{M'X}$ = 11.0 Hz, 2H), 3.47 – 3.42 (m, 2H, CHO), 2.95 (dd, another CH_2O protons in oxirane ring (H_M), J_{MA}=4.8, J_{MX} = 9.2 Hz, 2H), 2.83 (dd, one of another CH_2O protons in oxirane ring (H_A), J_{AX} =2.7, J_{AM} = 5.0 Hz, 2H), 1.89 – 1.72 (m, 3H, CH_2, CH), 1.07 (d, J = 6.3 Hz, 6H, CH_3). ^{13}C NMR (100 MHz, $CDCl_3$) δ (ppm): 152.7, 140.9, 139.3, 137.9, 129.0, 126.3, 125.0, 123.7, 123.1, 122.5, 120.7, 119.3, 119.2, 115.9, 110.8, 109.5, 108.9, 104.5, 70.1 (2C, OCH_2), 50.5 (2C, OCH), 44.9 (2C, OCH_2 in oxirane ring), 41.6 (NCH_2), 37.6 (CH), 26.2 (CH_2), 22.7 (2C, CH_3). MS (APCl$^+$, 20 V), *m/z* (%) = 547 ([M + H]$^+$, 100). Elemental analysis. Calcd for $C_{35}H_{34}N_2O_4$ (%): C 76.90, H 6.37, N 5.12, O 11.71; found (%): C 79.96, H 6.40, N 5.15. IR (KBr), ν, (cm^{-1}): 3061, 3014 (C-H, Ar); 2960, 2923, 2875 (C-H, Alif); 1603, 1577, 1494, 1485 (C=C, Ar); 1327 (C-N); 915, 845 (C-O-C); 749 (C-H, Ar).

*3-(3,6-Di(3-methyloxetane-3-yl-methoxy)carbazol-9-yl)-9-isopentylcarbazole (**7b**)*

Compound **6** (0.2 g, 0.46 mmol) was dissolved in ethylmethylketone (5 ml) and 3-bromomethyl-3-methyloxetane (0.46 g, 2.8 mmol) was added dropwise. After adding NaH (0.06 g, 2.8 mmol) the reaction was carried out at 60 ^{o}C for three hours. The excess of 3-bromomethyl-3-methyloxetane was removed at the reduced pressure and the obtained resin was dissolved in ethyl acetate, washed several times with water and dried over magnesium sulfate. The solvent was evaporated under vacuum and the crude product was purified by column chromatography on silica gel using hexane/ethyl acetate (1/8) as an eluent. The target compound was obtained as yellowish crystals (fw=602 g/mol, m.p.: 160 – 161 ^{o}C) in 64 % yield (0.18 g). ^{1}H NMR (400 MHz, $CDCl_3$), δ (ppm): 8.20 (s, 1H, Ar), 8.06 (d, J = 7.7 Hz, 1H, Ar), 7.65 (d, J = 2.4 Hz, 2H, Ar), 7.58 – 7.43 (m, 4H, Ar), 7.34 – 7.20 (m, 3H, Ar), 7.07 (dd, J = 8.8, 2.5 Hz, 2H, Ar), 4.73 (d, J = 5.9 Hz, 4H, CH_2O in oxetane ring), 4.51 (d, J = 5.9 Hz, 4H, CH_2O in oxetane ring),

4.39 (t, *J* = 7.6 Hz, 2H, N-CH_2), 4.18 (s, 4H, CH_2O), 1.88 – 1.72 (m, 3H, CH, CH_2), 1.51 (s, 6H, CH_3), 1.07 (d, *J* = 6.0 Hz, 6H). ^{13}C NMR (101 MHz, $CDCl_3$), δ (ppm): 153.3, 140.9, 139.3, 137.8, 129.1, 126.4, 125.0, 123.8, 123.1, 122.5, 120.7, 119.3, 119.2, 115.7, 110.8, 109.5, 108.9, 104.1, 80.0 (4C, OCH_2 in oxetane ring), 74.1 (2C, OCH_2), 41.6 (NCH_2), 39.9 (2C, CH in oxetane ring), 37.6 (CH), 26.2 (CH_2), 22.7 (2C, CH_3), 21.5 (2C, CH_3). MS ($APCl^+$, 20 V), *m/z* (%) = 603 ($[M + H]^+$, 100). Elemental analysis. Calcd for $C_{39}H_{42}N_2O_4$ (%): C 77.71, H 7.02, N 4.65, O 10.62; found (%): C 77.76, H 7.05, N 4.67. IR (KBr), ν, (cm^{-1}): 3056, 3031 (C-H, Ar); 2957, 2950, 2872 (C-H, Alif); 1606, 1575, 1494, 1471 (C=C, Ar); 1325 (C-N); 981, 935, 841 (C-O-C); 746 (C-H, Ar).

*3-(3,6-Di(2-(vinyloxy)ethoxy)carbazol-9-yl)-9-isopentylcarbazole (**7c**)*

Compound **6** (0.16 g, 0.37 mmol), 2-chloroethylvinylether (0.16 g, 1.5 mmol) and tetrabutylammonium hydrogen sulfate (TBAHS, 0.006 g, 0.02 mmol) were dissolved in acetone (15 ml). The mixture was heated to reflux and potassium hydroxide (0.12 g 2.2 mmol) as well as sodium sulfate (0.1 g, 0.72 mmol) were added. After refluxing for 2 hours, acetone was removed and the reaction product was dissolved in ethyl acetate and washed with water. The crude product was purified by column chromatography on silica gel using hexane/ethyl acetate (1/8) as an eluent. The target compound was obtained as white crystals (fw=574 g/mol, m.p.: 103 – 104 ^oC) in 52 % yield (0.11 g). ^{1}H NMR (400 MHz, $CDCl_3$), δ (ppm): 8.19 (s, 1H, Ar), 8.06 (d, *J* = 7.6 Hz, 1H, Ar), 7.62 (d, *J* = 2.4 Hz, 2H, Ar), 7.55 – 7.45 (m, 4H, Ar), 7.32 – 7.23 (m, 3H, Ar), 7.07 (dd, *J* = 8.9, 2.5 Hz, 2H, Ar), 6.60 (dd, *J* = 14.4, 6.8 Hz, 2H, OCH), 4.43 – 4.34 (m, 6H, NCH_2, OCH_2), 4.29 (dd, *J* = 14.4, 2.2 Hz, 2H, CH=C$\underline{H}_2$), 4.15 – 4.07 (m, 6H, CH=C$\underline{H}_2$, OCH_2), 1.87 – 1.71 (m, 3H, CH, CH_2), 1.07 (d, *J* = 6.3 Hz, 6H, CH_3). ^{13}C NMR (100 MHz, $CDCl_3$), δ (ppm): 152.7, 140.9, 139.2, 137.8, 129.1, 126.3, 125.0, 123.7, 123.1, 122.5, 120.7, 119.3, 119.2, 115.9, 110.8, 109.4, 108.9, 104.5, 86.9 (2C, CH=), 67.7 (4C, OCH_2), 66.6 (2C, CH_2=), 41.6 (NCH_2), 37.6 (CH), 26.2 (CH_2), 22.6 (2C, CH_3). MS ($APCl^+$, 20 V), *m/z* (%) = 575 ($[M + H]^+$, 100). Elemental analysis. Calcd for $C_{37}H_{38}N_2O_4$ (%): C 77.33, H 6.66, N 4.87, O 11.14; found (%): C 77.39, H 6.69, N 4.90. IR (KBr), ν, (cm^{-1}): 3058 (C-H, Ar); 2956, 2945, 2875 (C-H, Alif); 1606, 1573, 1490, 1463 (C=C, Ar); 1323 (C-N); 1151 (C-O-C), 1107, 962, 846 (CH=CH_2); 748 (C-H, Ar).

*General procedure of photocross-linking of monomers **7a–c***

Silicon glass slides were used as the substrates. The slides were carefully cleaned and dried before use. Solutions of the monomers **7a–c** in 1,2-dichloroethane (10 %) were prepared, and 3 mol% of diphenyliodonium hexafluorphosphate was added shortly before drop-casting. After drop-casting the samples were dried and then irradiated by UV lamp for 1 hour.

Polymer **P1** was obtained from monomer **7a** after photorosslinking. IR (KBr), ν, (cm^{-1}): 3061, 3014 (C-H, Ar); 2960, 2923, 2875 (C-H, Alif); 1603, 1577, 1494, 1485 (C=C, Ar); 1327 (C-N); 1106 (C-O-C); 749 (C-H, Ar).

P2 was obtained from monomer **7b** after photorosslinking. IR (KBr), ν, (cm^{-1}): 3056, 3031 (C-H, Ar); 2957, 2950, 2872 (C-H, Alif); 1606, 1575, 1494, 1471 (C=C, Ar); 1325 (C-N); 1047 (C-O-C); 746 (C-H, Ar).

P3 was obtained from monomer **7c** after photorosslinking. IR (KBr), ν, (cm^{-1}): 3058 (C-H, Ar); 2956, 2945, 2875 (C-H, Alif); 1606, 1573, 1490, 1463 (C=C, Ar); 1323 (C-N); 1151 (C-O-C); 748 (C-H, Ar).

3. Results and discussions

3.1. Synthesis

The cross-linkable monomers were synthesized by multi-step synthetic route as shown in Scheme 1. The first step was Tucker iodination of 9*H*-carbazole using KI and KIO_3. 3-Iodo-(9-isopentyl)carbazole (**2**) was obtained by alkylation of 3-iodocarbazole (**1**) with 1-bromo-3-methylbutane (BrMeBu). Ullman coupling reaction of iodocarbazole **2** with an excess of 3,6-dimethoxycarbazole (**4**) led to 3-(3,6-dimethoxycarbazol-9-yl)-9-isopentylcarbazole (**5**). Compound **4** was synthesized by bromination of 9*H*-carbazole with N-bromosuccinimide (NBS) in chloroform, followed by the direct methoxide displacement of bromine in 3,6-dibromo-9*H*-carbazole (**3**). Demethylation of methoxy groups of compound **5** using boron tribromide at -80 ^{o}C, gave compound **6** which was used for the synthesis of monomers **7a–c**.

Compound **7a** was obtained by the reaction of compound **6** with 3-chloro-1,2-epoxypropane using BTMA, whereas by interaction of **6** with 3-bromomethyl-3-methyloxetane or 2-chloroethylvinylether in the basic conditions gave **7b** and **7c**, respectively.

Scheme 1.

The structures of synthesized compounds were confirmed by ^{1}H and ^{13}C NMR, mass spectrometries, and elemental analysis. The cross-linkable compounds **7a**, **7b**, and **7c** were used for the preparation of the cross-linked materials **P1**, **P2**, and **P3** (Scheme 2).

Scheme 2.

The kinetics of consumption of reactive functional groups of **7a–c** were monitored by real-time FT-IR spectrometry. The samples were simultaneously exposed to UV irradiation beam and to the analyzing IR beam, which monitored the resulting drop of absorbance. The degree of conversion were calculated from the decrease of IR absorption bands of reactive functional groups according to equation:

$$Degree\ of\ conversion\ (\%) = ((A_0 - A_t)/A_0)\times 100;$$

where A_0 and A_t are optical density of absorption bands before and after UV irradiation for a certain period of time.

The IR absorption bands at 845 cm^{-1}, 981 cm^{-1}, 962 cm^{-1} were used to estimate the degree of conversion of epoxypropyl, oxetanyl and vinyloxyethyl groups, respectively. Fig 1 shows a stacked plot of IR spectra of the photopolymerization mixture of monomer **7a** over the reaction time period of 1 hour. The decrease of intensity of absortion bands at 845 and 910 cm^{-1} as function of time represents the rate of the consumption of the epoxypropyl groups, while the increase of the optical density of absorption band centered at 1100 cm^{-1} throughout the reaction period, identifies the increased number of C-O-C linkages. The similar trends were observed for polymerization of monomers **7b** and **7c**, where changes in optical density of characteristic absorbtion bands of epoxypropyl groups centered at 835, 941, 981 cm^{-1} and of vinyloxyethyl moieties at 844, 962, 1103 cm^{-1} were monitored in IR spectra (Figure S7 and S8 in). The optical density of the peak of absorption band of aromatic group at ca. 1460 cm^{-1} was used as internal standard for all kinetic calculations.

Fig 1.

High initial rate of cross-linking was observed during UV irradiation. After 5 min of irradiation, the degrees of conversion of epoxypropyl, oxetanyl and vinyloxyethyl groups reached ca. 48, 51 and 39 %, respectively. After 1 h, the highest conversion (ca. 78 %) was observed for epoxypropyl groups (Fig 2).

Fig 2.

3.2. Thermal properties

The thermal properties of the synthesized compounds were studied by DSC and TGA. The values of glass transition temperatures (T_g), melting point (T_m), and temperatures at which 5% loss of mass (T_{ID}) were observed are summarized in Table 1. All the synthesized compounds demonstrated relatively high thermal stability. The values of T_{ID} were found to be higher than 328 ^oC as confirmed by TGA at the heating rate of 10 ^oC/min. The increased molecular weight of polymers determined higher thermal stability compared to that of the corresponding monomers and T_{ID} values are higher by ca 40 ^oC.

Table 1

Formation of the glassy state of all synthesized compounds was confirmed by DSC analysis. The synthesized compounds **6**, **7b** and **7c** were obtained as crystalline materials. However, they readily formed glasses when their melt samples were cooled down. For the illustration of above stated the DSC curves of compound **6** are shown in Fig 3. The sample showed endothermic melting signal at 133 ^{o}C during the first heating cycle. It did not subsequently crystallize when cooled down, and exhibited a glass transition temperature of 98 ^{o}C during the second heating scan.

Fig 3.

Compounds **5**, **7a** and polymers **P1–P3** were isolated as amorphous materials. Only glass transition were observed in their DSC scans, and no peaks due to crystallization and melting appeared. Cooling and the following heating scans revealed only glass transition. The DSC curves of the second heating scans of polymers **P1–P3** and monomers **7a–c** are presented in Fig 4.

Fig 4.

T_g values of polymers **P1–P3** were found to be higher than those of the corresponding monomers. This observation can be explained by the increased molecular size of polymers. Among the low-molecular-weight compounds the highest T_g was observed for compound **6** containing hydroxyl groups (T_g = 98 ^{o}C), which apparently take part in hydrogen bonding. Replacement of hydrogen atoms by the epoxypropyl, oxethanyl or vinyloxethyl groups changes the lead to decreased packing density of the molecules. These conformational changes and the effect of the additional aliphatic chains of the functional groups apparently determined the lower T_g values of the monomers by 22 – 56 ^{o}C compared to that of compound **6**.

3.3. Optical and photophysical properties

The synthesized low-molecular-weight compounds exhibit similar photophysical properties because of their similar structures. UV absorption and fluorescence spectra of monomer **7a** are presented in Fig 5. The absorption spectrum covers the near-ultraviolet region (200 – 390 nm) and shows a narrow absorption band at 311 nm corresponding to the local π–π^* electron transition of a single carbazole moiety [22]. The carbazole moiety also contributes to the absorption bands at longer wavelengths (354 and

370nm); however, these bands in the UV spectra of compounds **5–7c** are significantly wider and red-shifted indicating optical transitions, which involve electron charge redistribution over the whole molecules consisting of two carbazole moieties [23].

Dilute THF solutions of the synthesized compounds exhibited blue emission with the intensity maxima at ca. 400 nm. The materials showed small Stokes shifts (30 nm) indicating low energy loss during the relaxation process.

Fig 5.

The phosphorescence spectra of the monomers were recorded at 77 K by applying delay time of 100 μs after excitation on purpose to evaluate the potential of the carbazole derivatives **5–7** and polymers **P1–P3** to be exploited as the host materials in phosphorescent OLEDs. Triplet state energies (E_T) estimated from the highest-energy peak of the phosphorescence spectra were found to be 2.78 eV. This value is higher than that of common blue phosphorescent emitter iridium(III)bis[(4,6-difluorophenyl)-pyridinato-N,$C^{2'}$]picolinate (FIrpic, E_T=2.65 eV) [24] and efficient energy transfer from the host to FIrpic dopant can be predicted, suggesting that the synthesized monomers **5–7** and polymers **P1–P3** can be suitable as the host materials for blue phosphorescent OLEDs.

3.4. Electrochemical and photoelectrical properties

The ionization potentials and electron affinities were established by cyclic voltamperometry (CV). The measurements were carried out with a glassy carbon electrode in dichloromethane solutions containing 0.1 M tetrabutylamonium perchlorate (TBAP) as electrolyte, $Ag/AgNO_3$ as the reference electrode and a Pt wire counter electrode. The experiments were calibrated with the standard ferrocene/ferrocenium redox system [25]. The cyclic voltammograms of all the studied compounds showed quasi-reversible oxidation couples. The electrochemical characteristics are summarized in Table 2. The synthesized carbazole derivatives have an open reactive C-6 position, however they exhibited stable redox properties and the formation of radical cations in the solutions did not lead to the creation of dimeric derivatives as it was earlier observed for 3-monosubstituted carbazole compounds [26]. This means that the substituent at the C-3 position of carbazole moity stabilizes radical cation [27]. As an example, several cyclic voltammogram scans of compound **5** are presented in Fig 6.

Fig 6.

The ionization potentials ($I_{p(CV)}$) of the synthesized monomers were found to be in the short range of 5.11 – 5.30 eV. The lowest value of $I_{p(CV)}$ was showed by compound **5** containing methoxy groups. With the

band gap (E_g^{opt}) values obtained from the absorption spectra, the electron affinity ($E_{A(CV)}$) values of **5–7** were calculated which range from 1,95 to 2,14 eV (Table 2).

The ionization potentials ($I_{p(EP)}$) of the solid layers of the monomers were estimated by the electron photoemission in air method. Compound **6** containing hydroxyl groups showed the highest ionization potential value of 5.37 eV. The ionization potential values of the other compounds (**5** and **7a–c**) were found to be comparable i.e. 5.20 – 5.29 eV (Table 2).

Table 2

The time-of-flight technique was used to characterize hole drift mobility in the amorphous films of **5**, **6** and **7a–c**. Compound **5** having methoxy groups exhibited slightly better charge-transporting properties. Hole drift mobility in solid film of **5** reached 1.3×10^{-5} cm^2/V, while films of other compounds demonstrated hole drift mobility in the range of $1.2 \times 10^{-6} – 4.8 \times 10^{-6}$ $cm^2/V \cdot s$ at electric field $E = 3.6 \times 10^5$ V/cm (Table 2). The hole drift mobilities of the studied compounds show linear dependencies on the square root of the electric field ($E^{1/2}$) with the good agreement to Poole–Frenkel relationship $\mu=\mu_0 \times exp(\alpha \times E^{1/2})$ (Figure 6) [28]. The values of the zero electric field charge mobility (μ_0) and the field dependence parameter (α) are given in Table S1 showing strong dependencies of μ on electric field. Compound **6** containing hydroxyl groups showed the lowest hole drift mobility, while the cross-linkable compounds **7a**, **7b**, and **7c** presented slightly higher mobilities (Figure 7). Distinctive plateau in the TOF transients is not clearly seen showing that hole transports of the compounds are dispersive (Figures S9-S13).

Fig 7.

4. Conclusions

New glass-forming carbazole dimers with reactive functional groups were synthesized. Their cationic photocross-linking was monitored by FT-IR spectrometry. The highest degree of conversion of reactive functional groups was observed for the monomer containing epoxypropyl groups. The molecular structure of the synthesized compounds allows them to exist in solid amorphous state. Their glass transition temperatures depend on the nature of the functional group. The highest glass transition temperature was observed for the compound containing hydroxyl groups (98 ^oC). Polymers exhibited considerably higher glass transition temperatures than monomers (89–150 ^oC). Dilute THF solutions of the synthesized compounds exhibited blue emission with the intensity maxima at ca. 400 nm. The electron photoemission

spectra of the solid layers of the monomers revealed ionization potentials of 5.54–5.61 eV. Hole drift mobility of the materials reached 1.3×10^{-5} $cm^2/V\cdot s$ at electric field of 3.6×10^5 V/cm, as established by time-of-flight technique.

Aknowledgement

This research was funded by a grant No. TAP LB-03/2015 from the Research Council of Lithuania.

References

[1] B. Wang, M.G. Helander, J. Qiu, D.P. Puzzo, M.T. Greiner, Z.M. Hudson, S. Wang, Z.W. Liu, Z.H. Lu, Unlocking the full potential of organic light-emitting diodes on flexible plastic. Nat. Photonics 5 (2011) 753−757.

[2] V. Bulovic, G. Gu, P.E. Burrows, S.R. Forrest, M.E. Thompson, Transparent light-emitting devices, Nature 318 (1996) 29.

[3] R.C. Kwong, S. Sibley, T. Dubovoy, M. Baldo, S.R. Forrest, M.E. Thompson, Efficient, saturated red organic light emitting devices based on phosphorescent platinum(II) porphyrins, Chem. Mater. 11 (1999) 3709.

[4] F. So, J. Kido, P. Burrows, Organic Light-emitting devices for solid-state lighting, MRS Bull. 33 (2008) 663.

[5] C.A. Zuniga, S. Barlow, S.R. Marder, Approaches to solution-processed multilayer organic light-emitting diodes based on cross-linking, Chem. Mater. 23 (2011) 658-681.

[6] S. Liu, X. Jiang, H. Ma, M.S. Liu, A.K.Y. Jen, Triarylamine-containing poly(perfluorocyclobutane) as a hole transporting-materials for polymers light-emitting diodes, Macromolecules 33 (2000) 3514–3517.

[7] X.Z. Jiang, S. Liu, M.S. Liu, P. Herguth, A.K.-Y. Jen, H. Fong, M. Sarikaya, Perfluorocyclobutane-based arylamine hole-transporting materials for organic and polymer light-emitting diodes, Adv. Funct. Mater. 12 (2002) 745–751.

[8] D.C. Müller, T. Braig, H.G. Nothofer, M. Arnoldi, M. Gross, U. Scherf, O. Nuyken, K. Meerholz, Efficient blue organic light-emitting diodes with graded hole-transporting layers, ChemPhysChem. 1 (2000) 207–211.

[9] E. Bacher, S. Jungermann, M. Rojahn, V. Wiederhirn, O. Nuyken, Photopatterning of crosslinkable hole-conducting materials for application in organic light-emitting devices, Macromol. Rapid Commun. 25 (2004) 1191–1196.

[10] N. Rehmann, D. Hertel, K. Meerholz, H. Becker, S. Heun, Highly efficient solution-processed phosphorescent multilayer organic light-emitting diodes based on small-molecule hosts, Appl. Phys. Lett. 91 (2007) 103507.

[11] H. Yan, P. Lee, N. R. Armstrong, A. Graham, G. Evmenenko, P. Dutta, T. J. Marks, High-Performance Hole-Transport Layers for Polymer Light-Emitting Diodes. Implementation of Organosiloxane Cross-Linking Chemistry in Polymeric Electroluminescent Devices, J. Am. Chem. Soc. 127 (2005) 3172–3183.

[12] Q. Huang, G. Evmenenko, P. Dutta, P. Lee, N.R. Armstrong, T.J. Marks, Covalently Bound Hole-Injecting Nanostructures. Systematics of Molecular Architecture, Thickness, Saturation, and Electron-

Blocking Characteristics on Organic Light-Emitting Diode Luminance, Turn-on Voltage, and Quantum Efficiency, J. Am. Chem. Soc. 127 (2005) 10227–10242.

[13] M.-H. Tsai, Y.-H. Hong, C.-H. Chang, H.-C. Su, C.-C. Wu, A. Matoliukstyte, J. Simokaitiene, S. Grigalevicius, J.V. Grazulevicius, C.-P. Hsu, 3-(9-Carbazolyl)carbazoles and 3,6-Di(9-carbazolyl)carbazoles as effective host materials for efficient blue organic electrophosphorescence, Adv.Mater. 19 (2007) 862-866.

[14] J.F. Morin, M. Leclerc, D. Adès, A. Siove, Polycarbazoles: 25 years of progress, Macromol. Rapid Commun. 26 (2005) 761-778.

[15] T. Malinauskas, M. Daskeviciene, K. Kazlauskas, H.C. Su, J.V. Grazulevicius, S. Jursenas, C.C. Wu, V. Getautis, Multifunctionalredphosphorescent bis-cyclometallatediridiumcomplexesbasedon 2-phenyl-1,2,3-benzotriazole ligandandcarbazolylmoieties, Tetrahedron 67 (2011) 1852-1861.

[16] C.A. Amorim, M.R. Cavallari, G. Santos, F.J. Fonseca, A.M. Andrade, S. Mergulhão, Determination of carrier mobility in MEH-PPV thin-films by stationary and transient current techniques, J. Non-Cryst. Solids 358 (2012) 484–491

[17] G. Juska, K. Genevicius, M. Viliunas, K. Arlauskas, H. Stuchlõkova, A. Fejfar, J. Kocka, New method of drift mobility evaluation in lc-Si:H, basic idea and comparison with time-of-light, J. Non-Cryst. Solids 266-269 (2000) 331-335.

[18] S.H. Tucker, LXXIV.—Iodination in the carbazole series, J. Chem. Soc. 129 (1926) 546-553.

[19] O. Stephen, J.-C. Vial, Blue light electroluminescent devices based on a copolymer derived from fluorene and carbazole, Synth. Met. 106 (1999) 115-119.

[20] Y. Kikugawa, Y. Aoki, T. Sakamoto, Synthesis of carbazoles from N-(N,N-diarylamino)phthalimides with aluminum chloride via diarylnitrenium ions, J. Org. Chem. 66 (2001) 8612-8615.

[21] J. M. Rodriguez-Parada, V. Percec, Interchain electron donor-acceptor complexes: a model to study polymer-polymer miscibility?, Macromolecules 19 (1986) 55.

[22] Z. Ge, T. Hayakawa, S. Ando, M. Ueda, T. Akiike, H. Miyamoto, T. Kajita, M. Kakimoto, Novel bipolar bathophenanthroline containing hosts for highly efficient phosphorescent OLEDs, Org. Lett. 10 (2008) 421.

[23] A. Tomkeviciene, J.V. Grazulevicius, K. Kazlauskas, A. Gruodis, S. Jursenas, T-H. Ke, C-C. Wu, Impact of linking topology on the properties of carbazole trimers and dimers, J. Phys. Chem. C 115 (2011) 4891-4892.

[24] R.J. Holmes, S.R. Forrest, Y.-J. Tung, R.C. Kwong, J.J Brown, S. Garon, M.E. Thompson, Blue organic electrophosphorescence using exothermic host-guest energy transfer, Appl. Phys. Lett. 82 (2003) 2422.

[25] M. Thelakkat, J. Ostrauskaite, A. Leopold, R. Bausinger, D. Haarer, Fast and stable photorefractive systems with compatible photoconductors and bifunctional NLO-dye, Chem. Phys. 285 (2002) 133.

[26] T.X. Lav, F. Tran-Van, F. Vidal, S. Peralta, C. Chevrot, D. Teyssie, J.V. Grazulevicius, V. Getautis, H. Derbal, J.M. Nunzi, Synthesis and characterization of p and n dopable interpenetrating polymer networks for organic photovoltaic devices, Thin Solid Films 516 (2008) 7223-7229.

[27] J.F. Ambrose, R.F. Nelson, Anodic oxidation pathways of carbazoles, J. Electrochem. Soc. 115 (1968) 1159.

[28] P.M. Borsenberger, J. Shi, Hole Transport in vapor deposited phenylenediamine molecular glass, Phys. Status Solidi B. 191 **(**1995) 461.

Figure captions

Scheme 1. Synthesis of monomers **7a-c**.

Scheme 2. Photocross-linking of monomers.

Fig 1. Progress of photopolymerization of **7a** and the spectral changes in the range 800-1600 cm^{-1} of the reaction mixture monitored by FT-IR.

Fig 2. Conversion of reactive functional groups versus time curves for photopolymerization of monomers **7a–c** initiated with DFIF. [DFIF] = 3 mol% of monomer.

Fig 3. DSC curves of **6** (scan rate 10 ^{o}C/min, N_2 atmosphere).

Fig 4. DSC curves of [A] monomers **7a–c** and [B] polymers **P1–P3** (scan rate 10 ^{o}C/min, N_2 atmosphere).

Fig 5. UV absorption and PL (λ_{ex} = 310 nm) spectra of dilute solution of compound **7a** (10^{-4} mol L^{-1}) in THF.

Fig 6. Cyclic voltammogram of **5** in argon-purged DCM solution (scan rate of 50 mV s^{-1}).

Fig 7. Hole drift mobilities as a function of $E^{1/2}$ for the layers of **5**, **6** and **7a–c**.

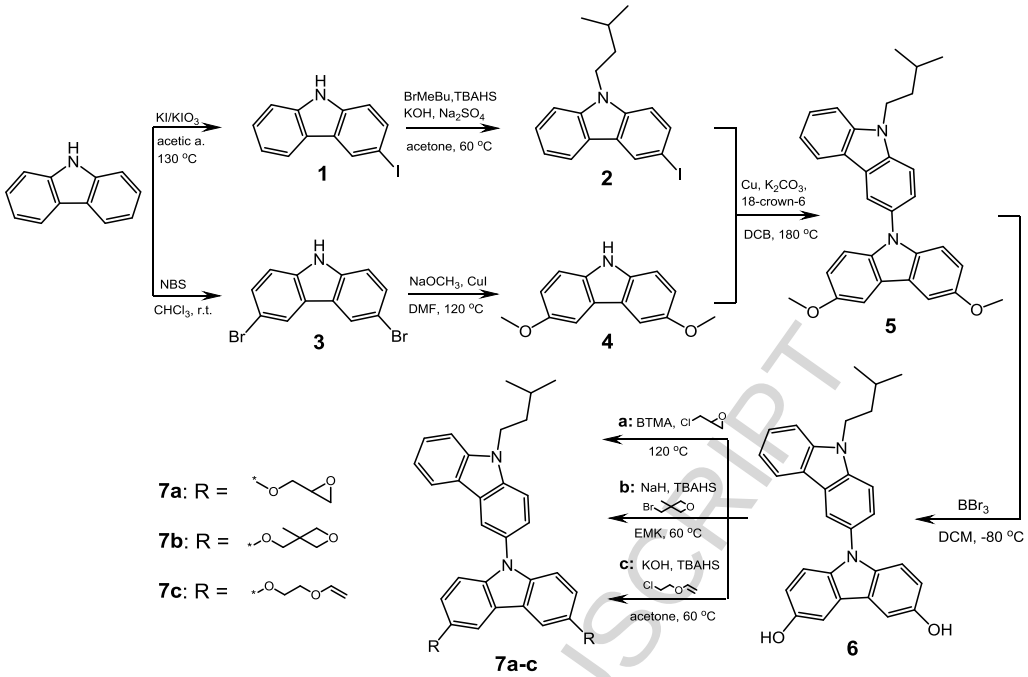

Scheme 1. Synthesis of monomers **7a-c**.

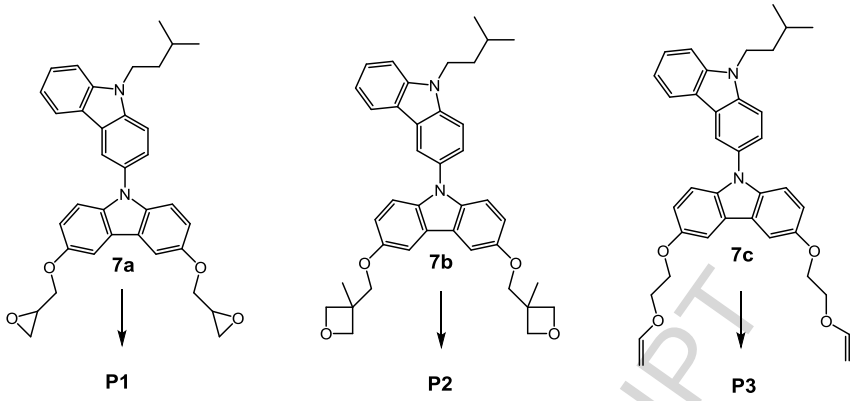

Scheme 2. Photocross-linking of monomers.

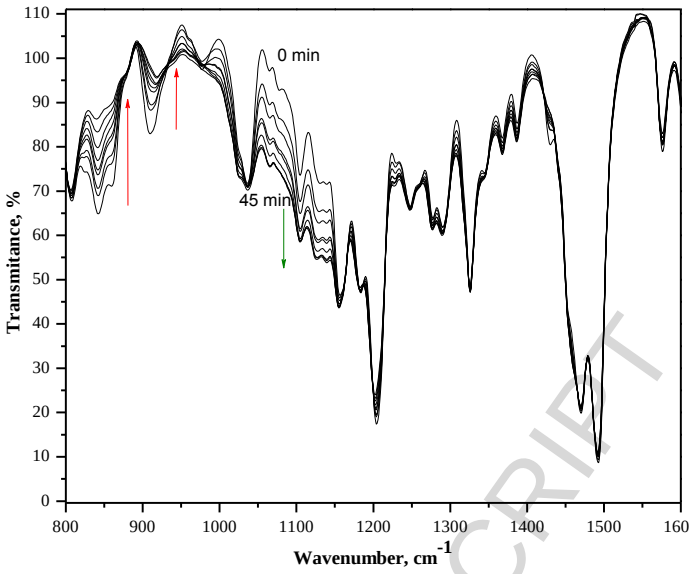

Fig 1. The spectral changes in the range of 800-1600 cm^{-1} of the photopolymerization mixture of **7a** monitored after the different periods of time (from 0 to 45 min) of irradiation by FT-IR.

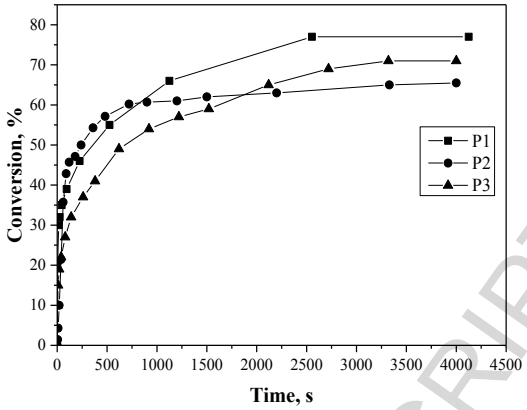

Fig 2. Conversion of reactive functional groups versus time curves for photopolymerization of monomers

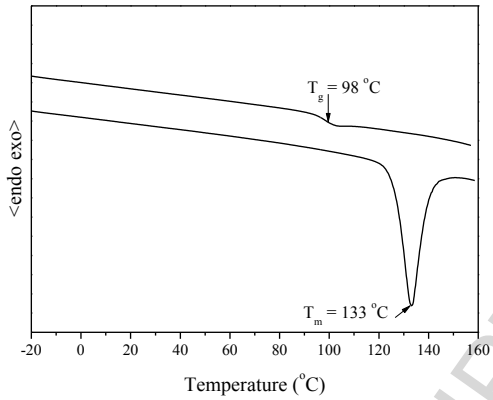

Fig 3. DSC curves of **6** (scan rate 10 ^{o}C/min, N_2 atmosphere).

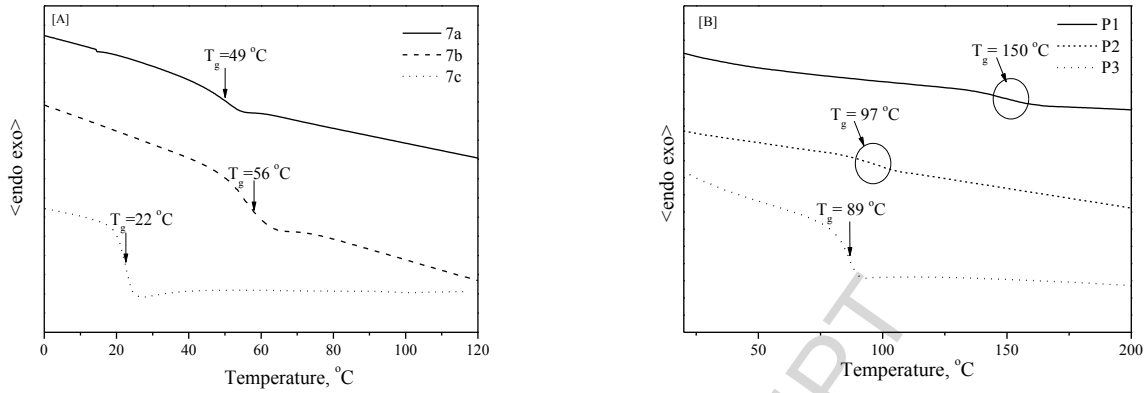

Fig 4. DSC curves of [A] monomers **7a–c** and [B] polymers **P1–P3** (scan rate 10 ^{o}C/min, N_2 atmosphere).

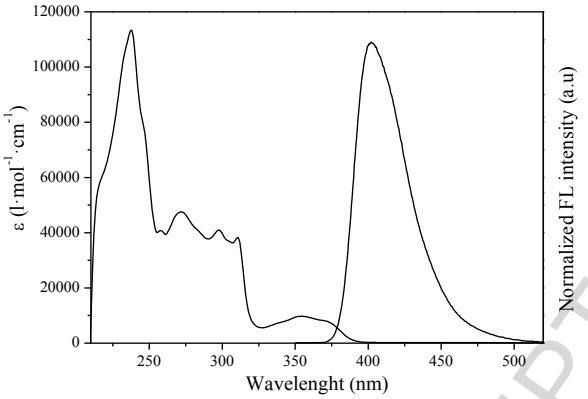

Fig 5. UV absorption and PL (λ_{ex} = 310 nm) spectra of dilute solution of compound **7a** (10^{-4} mol L^{-1}) in THF.

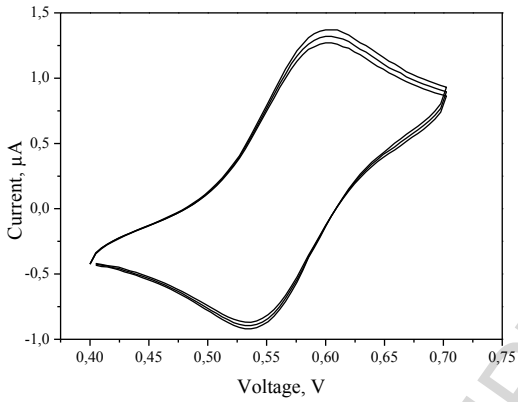

Fig 6. Cyclic voltammogram of **5** in argon-purged DCM solution (scan rate of 50 mV s^{-1}).

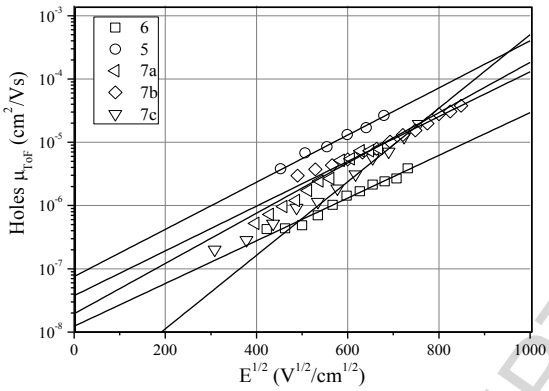

Fig 7. Hole drift mobilities as a function of $E^{1/2}$ for the layers of **5**, **6** and **7a–c**.

Table 1. Thermal characteristics of compounds **5**-**7c** and polymers **P1**-**P3**.

Compound	**5**	**6**	**7a**	**7b**	**7c**	**P1**	**P2**	**P3**
T_m, °C	-	133	-	161	103	-	-	-
T_g, °C	24	98	49	56	22	150	97	89
$T_{ID,}$ °C	335	360	328	337	355	375	382	379

Table 2. Electrochemical and photoelectrical characteristics of **5**, **6** and **7a–c**.

Compound	E_g^{opt} (eV)	$E_{1/2}$ (V)	$I_{p(CV)}$ [a] (eV)	$E_{A(CV)}$ [b] (eV)	$I_{p(EP)}$ [c] (eV)	μ [d] ($cm^2/V \cdot s$)
5	3.16	0.31	5.11	1.95	5.28	$1.3 \cdot 10^{-5}$
6	3.14	0.46	5.26	2.12	5.37	$1.2 \cdot 10^{-6}$
7a	3.16	0.44	5.24	2.08	5.28	$2.4 \cdot 10^{-6}$
7b	3.15	0.41	5.21	2.06	5.29	$4.8 \cdot 10^{-6}$
7c	3.16	0.50	5.30	2.14	5.20	$4.7 \cdot 10^{-6}$

[a] Ionization potentials $I_{p(CV)}$ and [b] electron affinities $E_{A(CV)}$ were estimated by cyclic voltamperometry according to $I_{p(CV)} = 4.8 + E_{1/2}$ and $E_{A(CV)} = -(I_{p(CV)} - E_g^{opt})$. [c] Ionization potentials $I_{p(EP)}$ were measured by electron photoemission spectrometry in air. [d] Hole mobility value at electric field $E = 3.6 \times 10^5$ V/cm.